JOURNAL OF BACTERIOLOGY, July 2004, p. 4585–4595 Vol. 186, No. 14
0021-9193/04/$08.00+0 DOI: 10.1128/JB.186.14.4585–4595.2004

Bacillus subtilis YdiH Is a Direct Negative Regulator of the *cydABCD* Operon

Matthew Schau, Yinghua Chen, and F. Marion Hulett*

Laboratory for Molecular Biology, Department of Biological Sciences, University of Illinois at Chicago, Chicago, Illinois 60607

Received 27 February 2004/Accepted 9 April 2004

During aerobic respiration, *Bacillus subtilis* utilizes three terminal oxidases, cytochromes aa_3, caa_3, and *bd*. Cytochrome *bd* is encoded by the *cydABCD* operon. We report here the first identification of a regulator for the *cydABCD* operon, YdiH. While working with Δ*resDE* mutant strains, we identified colonies which contained suppressor mutations (*cmp*) which bypassed the requirement for ResD for all phenotypes not associated with cytochrome aa_3 or caa_3. Mapping identified a class of Tn*10* insertions which were close to the *cmp* locus (Tn*10-2*) and a second class (Tn*10-1*) which was inserted in *cydD*, a gene which appears to be essential to the *cmp* phenotype. Sequencing of the *cmp* loci from four independent Δ*resDE cmp* isolates yielded four loss-of-function alleles of *ydiH*, a gene encoding a protein with homology to AT-rich DNA-binding proteins. Additionally, we determined that cytochrome *bd* was aberrantly expressed in the Δ*resDE cmp* background. Together these data led to the hypothesis that YdiH serves as a negative regulator of *cydABCD* expression, a hypothesis supported by both gel-shift and DNase I footprinting analyses. YdiH protected the *cydA* promoter region at three 22-bp repeats located in the long 5′ untranslated region (193 bp). Induction of the *cydABCD* operon in a Δ*resDE* background showed that expression of the terminal oxidase *bd* was responsible for the bypass phenotype observed in a Δ*resDE cmp* strain, indicating that cytochrome *bd* expression complemented the loss of cytochromes aa_3 and caa_3 in the Δ*resDE* strain.

Bacillus subtilis utilizes a branched electron transport chain under aerobic conditions. To date, three terminal oxidases have been identified in *B. subtilis*. Both cytochromes aa_3 (26) and caa_3 (5) have been identified as heme-copper oxidases. The third oxidase has been shown to be a member of the cytochrome *bd* family (35). The *cydABCD* operon of *B. subtilis* encodes cytochrome *bd* and a putative ABC transporter required for the production of functional cytochrome *bd* (35). This oxidase is produced under conditions of low oxygen tension and in cells grown in the presence of glucose (35). A single *cydA* transcriptional start site with a putative −10 and −35 consensus for a σ^A promoter has been found in cells grown to stationary phase in nutrient sporulation medium with phosphate buffer and glucose (NSMPG) (35). A perfect 16-bp palindromic sequence, upstream of the translation start site for *cydA*, was proposed as a potential operator binding site for a regulatory protein (35). To date, no regulators have been reported for the *cydABCD* operon. It was originally reported that the quinol oxidases (either cytochrome aa_3 or *bd*), are required for aerobic growth in *B. subtilis* (34). However, further evidence has shown that a strain deficient in the production of both cytochrome aa_3 and cytochrome *bd*, a derivative of the *B. subtilis* 168 strain (24), can be constructed and grown aerobically (37). A putative fourth terminal oxidase, YthAB, has been found in *B. subtilis* and is a member of the cytochrome *bd* family (34).

YdiH was identified during the course of sequencing the *B. subtilis* genome. Based on homology, YdiH was proposed to be a member of a family of AT-rich DNA-binding proteins (16) that includes p25, a recently characterized DNA-binding protein from *Thermus aquaticus* YT-1 (6).

The ResD/ResE two-component signal transduction system plays a role in the regulation of both aerobic respiration and anaerobic respiration. ResD regulates the expression of *fnr* (21), *hmp* (21), *nasDEF* (21), *hemN* (12), *hemZ* (12), and the *sbo-alb* operon (20) under anaerobic conditions and has a role in the regulation of *ctaA* (23, 38), *ctaBCDEF* (17), *resABCDE* (31), and *petCBD* (31) under aerobic conditions. Because ResDE is essential for expression of both *ctaA* and *ctaB*, which is required for heme A biosynthesis, Δ*resDE* strains lack cytochromes aa_3 and caa_3.

In the course of our work with Δ*resDE* strains, we have found that these strains develop secondary mutations which have been given the designation *cmp* mutations. The Δ*resDE* strains bearing the *cmp* mutation are complemented for a number of phenotypes typically associated with a Δ*resDE* strain. In the course of identifying and characterizing these *cmp* mutations, we have implicated YdiH, a previously uncharacterized putative DNA-binding protein, in the regulation of the *cydABCD* operon. In this paper, we report the characterization of YdiH as a negative regulator for *cydABCD* transcription. Additionally, we show that the absence of terminal oxidases in the Δ*resDE* strain is responsible for a number of phenotypes previously reported for that strain.

MATERIALS AND METHODS

Strains and plasmids. Table 1 lists the strains and plasmids used in this study. *Escherichia coli* DH5α was the host for all plasmid constructions. *E. coli* BL21(DE3)/pLysS (Novagen) served as the host for overexpression of the YdiH protein. *B. subtilis* JH642 served as the host for all strain constructions.

cydA-lacZ promoter fusions were constructed in pDH32, which has unique

* Corresponding author. Mailing address: Laboratory for Molecular Biology, Department of Biological Sciences, University of Illinois at Chicago, 900 S. Ashland Ave. (M/C 567), Chicago, IL 60607. Phone: (312) 996-5460. Fax: (312) 413-2691. E-mail: Hulett@uic.edu.

TABLE 1. Bacterial strains and plasmids used in this study

Strain or plasmid	Relevant characteristic	Source or reference
Strains		
E. coli		
DH5α		Lab stock
BL21(DE3)pLysS		Novagen
Bacillus		
JH642	*pheA1 trpC2*	J. A. Hoch
1A601	*purB83*::Tn*917* Mls^r	33
Δ*tatCY*-Δ*tatCD*	Δ*tatCY*::Spc^r Δ*tatCD*::Kn^r	14
MH1562	*phoB*::Tn*917* Mls^r	15
MH5202	*pheA1 trpC2* Δ*resDE*::Tet^r	31
MH5857	*pheA1 trpC2* Δ*resDE*::Tet^r *cmp amyE*::*phoD-lacZ* Cm^r	This study
MH5859	*pheA1 trpC2* Δ*resDE*::Tet^r *cmp amyE*::*phoD-lacZ* Cm^r	This study
MH5863	*pheA1 trpC2 ydhQ*ΩpMS7 Erm^r	This study
MH5867	*pheA1 trpC2 rrnE-23s*::Tn*10-2* Spc^r *ydhQ*ΩpMS7 Erm^r	This study
MH5874	*pheA1 trpC2* Δ*tatCY*::Spc^r *rrnE-23s*::Tn*10-2* Kn^r	This study
MH5878	*pheA1 trpC2 amyE*::pMS35*cydA-lacZ* Cm^r	This study
MH5879	*pheA1 trpC2* Δ*resDE*::Tet^r *cmp amyE*::*cydA-lacZ* Cm^r	This study
MH5880	*pheA1 trpC2* Δ*resDE*::Tet^r *amyE*::*cydA-lacZ* Cm^r	This study
MH5881	*pheA1 trpC2 ydhQ*Ω*pMS7* Erm^r *tatCY*::Spc^r	This study
MH5882	*pheA1 trpC2 cydD*::Tn*10-1* Spc^r Δ*resDE*::Tet^r *cmp*	This study
MH5883	*pheA1 trpC2 rrnE-23s*::Tn*10-2* Spc^r Δ*resDE*::Tet^r	This study
MH5884	*pheA1 trpC2* JH642ΩpMS38	This study
MH5885	*pheA1 trpC2* MH5884 Δ*resDE*::Tet^r	This study
MH5887	*pheA1 trpC2* Δ*resDE*::Tet^r *cmp*	Guofu Sun
MH5888	*pheA1 trpC2* Δ*resDE*::Tet^r *cmp*	Ruth Chestnut
MH5889	*pheA1 trpC2* Δ*tatCY*::Spc^r	This study
MH5890	*pheA1 trpC2 rrnE-23s*::Tn*10-2* Kn^r	This study
MH5891	*pheA1 trpC2 ydiH*Ω*pMS45* Spc^r *amyE*::*cydA-lacZ* Cm^r	This study
MH5893	*pheA1 trpC2* Δ*resDE*::Tet^r *ydiH*Ω*pMS45* Spc^r *amyE*::*cydA-lacZ* Cm^r	This study
Plasmids		
pCR2.1	Vector for cloning PCR products	Invitrogen
pIC333	Vector for Tn*10* mutagenesis, Spc^r Erm^r	29
pDH32	Vector for construction of promoter-*lacZ* fusions; Amp^r Cm^r	28
pAT110	Vector for mutant generation; Erm^r	32
pDG1727	Vector for mutant generation; Spc^r	9
pVK73	Antibiotic switching vector from Spc^r to Kn^r	3
pET16b	Vector for protein overexpression and His-tagging Amp^r	Novagen
pMS4	Internal fragment of *ydhQ* in pCR2.1	This study
pMS7	Fragment of *ydhQ* in pAT110; Erm^r Amp^r	This study
pMS34	Fragment of *cydA* promoter in pCR 2.1; Amp^r	This study
pMS37	Fragment of *cydA* in pCR2.1; Amp^r	This study
pMS38	P_{spac}-*cydABCD* in pDH88; Amp^r Cm^r	This study
pMS35	*cydA-lacZ* fusion in pDH32; Amp^r Cm^r	This study
pMS40	Internal fragment of *ydiH* in pCR2.1; Amp^r	This study
pMS45	Internal fragment of *ydiH* in pDG1727; Amp^r Spc^r	This study
pMS41	Coding sequence of *ydiH* in pCR2.1; Amp^r	This study
pMS43	Coding sequence of *ydiH* in pET16b; Amp^r	This study

EcoRI and BamHI sites upstream of a promoterless *lacZ* gene to correctly orient the promoter DNA fragment. Primers FMH741 (5′-CCGAATTC^{-305}TAGCA GCCGACATAAATAAG^{-285}-3′; EcoRI site underlined) and FMH742 (5′-CC GGATCC^{7}CACTCATGCTTTCTCCTCC ATTTCC^{-18}-3′; BamHI site underlined) were used to amplify a 312-bp fragment of the *cydA* promoter region spanning from −305 to +7 relative to the start of translation of CydA, using JH642 chromosomal DNA as template. The resulting fragment was ligated into pCR2.1 (Invitrogen) to create pMS34. The *cydA* promoter fragment was released from pMS34 by digestion with EcoRI and BamHI and cloned into the EcoRI and BamHI sites of pDH32 to create pMS35. DNA sequencing confirmed the sequence of the *cydA* promoter. MH5878 (*cydA-lacZ*) was created by transformation of JH642 with pMS35 linearized by digestion with PstI such that the promoter fusion was integrated into the *amyE* locus by double-crossover homologous recombination. Transformants were selected on chloramphenicol, and the required insertion was confirmed by the *amyE* mutant phenotype. Transformation of chromosomal DNA from MH5878 (*cydA-lacZ*) to MH5887 (Δ*resDE cmp*) produced MH5879 (*cydA-lacZ* Δ*resDE cmp*). Transformation of chromosomal DNA from MH5202 (Δ*resDE*) into MH5878 (*cydA-lacZ*) produced MH5880 (*cydA-lacZ* Δ*resDE*).

To create a mutation in *ydiH*, we cloned an internal fragment of the gene to pDG1727, which allows for the creation of an insertion-duplication mutation. Primers FHM788 (5′-$^{-42}$ACGGCTGCCGCTTTACTATC^{62}-3′) and FHM789 (5′-^{557}TGTTCCGG CACATTCAAACG^{537}-3′) were used to amplify a 516-bp internal fragment of *ydiH*, using JH642 chromosomal DNA as a template. The resulting PCR product was cloned to pCR2.1 to create pMS40. The *ydiH* fragment was released from pMS40 by digestion with EcoRV and BamHI and cloned into the EcoRV and BamHI sites of pDG1727 to create pMS45. pMS45 was transformed to MH5878 (*cydA-lacZ*) to create MH5891 (Ω*ydiH cydA-lacZ*). MH5893 (Ω*ydiH* Δ*resDE cydA-lacZ*) was created by transforming chromosomal DNA from MH5202 (Δ*resDE*) into MH5891 (Ω*ydiH cydA-lacZ*).

Inducible expression of the *cydABCD* operon was achieved by cloning in pDH88, which contains an isopropyl-β-D-thiogalactopyranoside (IPTG)-induc-

ible P_{spac} promoter. Primers FMH764 (5′-CCAAGCTT^{-23}TAACCGGAAATG GAGGAG^{-5}-3′; HindIII site underlined) and FMH765 (5′-CCGCATCG^{307}A CGCCAATAATTGCTTCAATC^{286}-3′; SphI site underlined) were used to amplify a 346-bp fragment containing positions −23 to +307 relative to the initiation of translation of CydA. This fragment contains the ribosome binding site for the *cydABCD* operon. The resulting PCR product was cloned to pCR2.1 to create pMS37. The *cydA* fragment was released from pMS37 by digestion with HindIII and SphI and cloned into complementary sites in pDH88 to yield pMS38. pMS38 was transformed to JH642 to yield MH5884 (P_{spac}-*cydABCD*). Transformation of chromosomal DNA from MH5202 (Δ*resDE*) to MH5884 (P_{spac}-*cydABCD*) yielded MH5885 (Δ*resDE* P_{spac}-*cydABCD*).

Due to the high rate of appearance of spontaneous suppressor mutations in a Δ*resDE* background, special precautions were taken in the constructions of all strains bearing a *resDE* mutation. Chromosomal DNA from MH5202 (Δ*resDE*) was used to transform the appropriate background whenever a strain with a *resDE* mutation was required. This was done to avoid the isolation of strains with *cmp* mutations during the production of competent cells of MH5202 (Δ*resDE*). All transformants were screened to confirm that the correct phenotype was present for each construction.

In order to create a mutation in *ydhQ*, we cloned an internal fragment of *ydhQ* to pAT110 in order to allow the creation of an insertion-duplication mutant. Primers FMH476 (5′-^{107}TTAACTCAAGCCGATGACG^{136}-3′) and FMH477 (5′-^{580}CCAGATG CTGCTGGTCAATA^{560}-3′) were used to amplify a 476-bp internal fragment of *ydhQ*. The resulting PCR product was cloned to pCR2.1 to create pMS4. The *ydhQ* fragment was released from pMS4 by digestion with NotI and HindIII and cloned into to NotI and HindIII sites of pAT110 to create pMS7. pMS7 was transformed to JH642 to yield MH5863 (Ω*ydhQ*). MH5889 (Δ*tatCY*) was created by transforming chromosomal DNA from Δ*tatCY*-Δ*tatCD* to JH642 and selecting on spectinomycin. Transformants were screened on plates containing kanamycin to confirm the single mutation. MH5881 (Δ*tatCY* Ω*ydhQ*) was generated by transforming chromosomal DNA from MH5863 (Ω*ydhQ*) into MH5889 (Δ*tatCY*).

MH5890 (*rrnE-23S*::Tn*10-2* Kn^r) was created by transforming the antibiotic-switching vector pVK73 into MH5883 (*rrnE-23S*::Tn*10-2* Spc^r) and selecting on kanamycin. Transformants were screened for spectinomycin sensitivity to confirm that the antibiotic switch was successful. Transformation of chromosomal DNA from MH5889 (Δ*tatCY*) to MH5890 (*rrnE-23S*::Tn*10-2*) yielded MH5874 (Δ*tatCY rrnE-23S*::Tn*10-2*).

To construct a plasmid for overexpressing YdiH, we amplified the entire coding sequence of *ydiH* by using the primers FMH790 (5′-TACATATGAAT AAGGATCAATCAAAAATTCCGCAGGCGA-3′; NdeI site underlined) and FMH791 (5′-TAGGATCCCTATTCGATTTCCTCTAAAACTGAATAATGC-3′; BamHI site underlined). JH642 was used as the template for PCR. The resulting PCR product was cloned to pCR2.1 to create pMS41. After DNA sequence confirmation, the coding sequence of *ydiH* was released from pMS41 by digestion with NdeI and BamHI and cloned to the NdeI and BamHI sites of pET16b to create pMS43. pMS43 was transformed to *E. coli* BL21(DE3)/pLysS, and representative transformants were used for overexpression of the YdiH protein.

Genetic manipulations. Transformation of *B. subtilis* was by the two-step transformation method of Cutting and Vander Horn (4). Transformants were selected on tryptose blood agar base medium (TBAB) supplemented with 0.5% glucose (TBABG) and the appropriate antibiotic. Antibiotics were added to the medium for selection of *B. subtilis* transformants at the following concentrations: chloramphenicol, 5 μg/ml; erythromycin, 1 μg/ml; spectinomycin, 100 μg/ml; tetracycline, 10 μg/ml; kanamycin, 10 μg/ml; and erythromycin, 1 μg/ml, and lincomycin, 25 μg/ml (mls). Preparation of PBS1 transducing lysates and PBS1 transduction were performed by the method of Cutting and Vander Horn (4). Transductants were selected on TBABG plates with the appropriate antibiotic at the concentrations listed above. Transformation of *E. coli* was done according to the method of Hanahan (10). Transformants were selected on Luria-Bertani (LB) plates containing ampicillin (100 μg/ml).

The plasmid pIC333 was used as the source for Tn*10* mutagenesis. Transposition was performed in the wild-type (JH642) background following the method of Steinmetz and Richter (29). Chromosomal DNA from the Tn*10* library was used to transform MH5857 (Δ*resDE cmp*). These transformants were picked to TBAB, TBABG, TBABG-spectinomycin, TBABG-chloramphenicol, and TBABG-tetracycline plates. Any Tn*10* insertion that cotransformed with a wild-type copy of the *cmp* locus was identified based on the reversion from the Δ*resDE cmp* phenotype to the Δ*resDE* phenotype on TBAB and TBABG plates. Further confirmation of a Tn*10* insertion near the *cmp* locus was obtained by backcross transformation of Tn*10* to a strain bearing the *cmp* mutation in order to determine the frequency at which each Tn*10* was linked to the wild-type copy of the *cmp* locus. This frequency was based on the number of Tn*10*-bearing transformants that reverted from the Δ*resDE cmp* phenotype to the Δ*resDE* phenotype on plates.

Growth conditions and enzyme assays. Growth for measurement of *cydA-lacZ* expression was performed in LB medium supplemented with 0.5% glucose. β-Galactosidase activity was detected by the method of Ferrari et al. (8). One activity unit was defined as 0.33 nmol of *o*-nitrophenol produced min^{-1}, and the specific activity was calculated as activity per milligram of protein. When appropriate, IPTG was added at a final concentration of 1 mM to the medium. Alkaline phosphate (alkaline phosphatase) activity was measured in cells that had been grown in low-phosphate defined medium (LPDM) as described previously (13).

Phenotypic characterization of mutant strains. The percentage of heat-resistant spores was determined by the method of Nicholson and Setlow (22). Cytochrome oxidase activity was assayed with TMPD as a substrate as previously described by Muller and Taber (18). Organic acid production was measured on purification agar medium plates by the method of Carls and Hanson (2). Anaerobic growth on plates was carried out in a BBL GasPak jar with BBL GasPak anaerobic system chemicals added according to the manufacturer's instructions. TBABG plates supplemented with 0.2% KNO_3 were used as the medium for anaerobic growth.

Preparation and spectrophotometry of solubilized membrane vesicles. Membrane vesicles were prepared as described by Bisschop and Konings (1), with the following modifications. Cells were collected from stationary-phase cultures grown in LB medium with 0.5% glucose. DNase and RNase were omitted from the lysis procedure. Solubilization of cytochromes and analysis of difference absorption spectra were performed as described by Mueller and Taber (18). Difference absorption spectra (dithionite reduced minus ferricyanide oxidized) were recorded at room temperature at a scan speed of 5 nm/s with a Hitachi U-2000 spectrophotometer. Reduction and oxidation were performed as previously described (18).

Inverse PCR. In order to determine the site of each Tn*10* insertion, inverse PCR was performed. Chromosomal DNA from MH5882 (Tn*10-1*) or MH5883 (Tn*10-2*) was subjected to digestion with PstI. Following digestion, each sample was ethanol precipitated and diluted to 10 μl in T4 DNA ligase buffer and treated with T4 DNA ligase overnight to allow for self-ligation. PstI cuts once within the Tn*10* insertion and then will cut the chromosomal DNA adjacent to the Tn*10* insertion at the next PstI site. The resulting product was used as the template in a two-step inverse PCR. Based on the sequence of pIC333, two sets of primers were developed complementary to each end of the Tn*10* remaining. FMH442 (5′-GCTATATCCAGTAAAGTTACAT-3′) and FMH443 (5′-GTGG GAAGGACTATATTCA-3′) were used in the first step of the PCR process. The product generated by these primers was diluted and used as the template for a second PCR. FMH446 (5′-ACATGCTCTTTAGGTA-3′) and FMH447 (5′-CC TCTTGTGAAATTAG-3′) were used to generate the second PCR product. The resulting PCR product was purified following the manufacture's instructions for the Microcon PCR kit (Millipore). DNA sequencing of the purified PCR products was performed by the University of Chicago Cancer Research Sequencing Center. In order to confirm the insertion of Tn*10-1* in *cydD*, we performed PCR with FMH438 (5′-AGCGAGTCAGTGAGCGAGGA-3′) complementary to Tn*10* and FMH782 (5′-CGGAGCTGGTGAACAACCTT-3′) complementary to positions −372 to −352 of *cydD*, using MH5882 as the template for the PCR. The resulting PCR product was purified and sequenced, confirming the insertion of Tn*10-1* in *cydD*. In order to confirm the insertion of Tn*10-2* in *rrnE-23S*, we again used FMH438, which was paired with FMH783 (5′-CCGTGTGCCTACC TACAAGTAGTC-3′) complementary to positions 563 to 583 of *rrnE-23S*, using MH5883 as the template for PCR. Again the resulting PCR product was purified and sequenced, confirming the insertion of Tn*10-2* in *rrnE-23S*.

PCR identification of the *cmp* locus. In order to identify the locus of the *cmp* mutation, we designed 15 pairs of PCR primers spanning the region from 88 bp upstream of the start of translation of *thiL* to 98 bp into the coding sequence of *tatCY*. The sequence and position of all primers used to identify the *cmp* locus are found in Table 2. These primers were used to amplify 15 overlapping PCR fragments, using MH5857 as the template DNA. All PCRs were performed in triplicate, and the resulting products were purified with the Microcon PCR purification kit. The resulting PCR products were sequenced, and the sequence was compared to the published genome sequence for each region. The corresponding protein sequence for all mutations found was determined with Clone Manager (SciEd Central) and compared to the wild-type protein sequence for the given locus obtained from the *B. subtilis* genome sequence database, SubtiList (http://genolist.pasteur.fr/SubtiList/).

Overexpression and purification of YdiH. *E. coli* BL21(DE3)pLysS harboring pMS43 was incubated overnight at 37°C in LB medium containing ampicillin

TABLE 2. Primers used of the identification of the *cmp* locus

Primer	Sequence (5′ → 3′)	Starting location (bp)
FMH617	CGGGAACATCTTGGATAAT	−88 of *thiL*
FMH618	TCCGTCACTAACATCATTT	637 of *thiL*
FMH619	GCCTGAGCCAAGAGTAAGC	581 of *thiL*
FMH620	GTCGGACTGTTTACAATACG	165 of *ydiB*
FMH621	GGAGACGTCCTGACATTAGA	191 of *ydiB*
FMH622	GCGGTGCCATATCACAATCAT	142 of *ydiC*
FMH623	GCGCTGCTTCGAGAAGACAC	45 of *ydiC*
FMH624	GCCAGCCGCAAGTAATCCG	634 of *ydiC*
FMH625	GCGCCTTCAGAATTGGCTT	608 of *ydiC*
FMH626	GCAGTCTCATCACAGCTTGTT	38 of *gcp*
FMH627	CGCTTGAAGTGAGGTTTCG	316 of *ydiD*
FMH628	CGGTCCACCCGGATATGGC	539 of *gcp*
FMH629	GCGGCAGGAGAAGCCTAC	495 of *gcp*
FMH630	CCTCAGCCCTTTATCCATCAA	+104 *gcp*
FMH649	CGCTCCTTAAACAGATCATA	−118 of *ydiF*
FMH650	GGCTTTGAACCTGTGTAGA	469 of *ydiF*
FMH651	GGCGGTTATCAATATGAAGC	399 of *ydiF*
FMH652	GAGCATGAATGACACTTCTG	1040 of *ydiF*
FMH653	CAGAGCGGAAATGAAGTCCT	961 of *ydiF*
FMH654	GGGTCACATAGCAATTCATC	1811 of *ydiF*
FMH655	CCAACGACTCCGTCGGATT	1722 of *ydiF*
FMH656	CCCATTCGGACAAAAGAGATT	1903 of *ydiF*
FMH657	CAGCTGATTAGCTTGTAAGAT	7 of *ydiF*
FMH658	GCGCTTCCATTTCCACAC	335 of *ydiG*
FMH659	GTGCCATCCGCTTTCATTG	225 of *ydiG*
FMH660	CGGATGATACACGCTGTT	109 of *ydiH*
FMH661	CGGCTGCCGCTTTACTATCG	43 of *ydiH*
FMH662	CGGCATATTTGGGCTCCTC	6 of *tatAY*
FMH663	GGTCGGCATTAGGAATCAAG	494 of *ydiH*
FMH664	GCGCTACAATCAGCAACC	79 of *tatCY*

(100 μg/ml) and was used to inoculate 1 liter of the same medium at a ratio of 1 to 100. The cells were grown at 30°C until the optical density at 600 nm (OD_{600}) of the culture reached about 0.4. IPTG was then added to the culture at a final concentration of 1 mM, and growth continued for another 3 h. The cells were harvested by centrifugation (5,000 × *g*) at 4°C and washed once with buffer A (1 M NaCl, 5 mM $MgCl_2$, 10 mM dithiothreitol [DTT], 50 mM Tris-HCl [pH 7.8]). The cell pellets were then suspended in 50 ml of prechilled buffer A on ice, containing 1 mM phenylmethlysulfonyl fluoride) and were immediately subjected to sonication. The disruption of cells was confirmed by phase-contrast microscopy. After centrifugation at 40,000 × *g* for 1 h at 4°C, the supernatant fraction was filtered through a 0.45-μm-pore-size membrane (Amicon). After adding a 1/50 volume of 0.5 M imidazole in buffer A, the clear cell lysate was mixed with a 2-ml Ni-nitrilotriacetic acid (NTA) (QIAGEN) affinity resin, preequilibrated with buffer A. After gentle shaking at 4°C for 30 min, the mixture was loaded onto an Econo column (inside diameter, 2.5 cm; height, 10 cm; Bio-Rad). The column was washed with buffer A until the elute contained nondetectable protein concentrations according to a Bio-Rad protein assay. The protein bound to the Ni-NTA resin was eluted by using 300 mM imidazole in buffer A. The protein fractions were dialyzed stepwise at 4°C against buffer A containing 20% glycerol with decreasing concentrations of NaCl from 1 M to 0.8, 0.6, 0.4, 0.2, and finally 0.1 M. The purity of YdiH proteins was over 95% as judged by sodium dodecyl sulfate-polyacrylamide gel electrophoresis (SDS-PAGE).

Preparation of *cydA* promoter probe. Primers FMH792 and FMH793 were end labeled with T4 polynucleotide kinase (Fermentas) in the presence of [γ-^{32}P]ATP, separated by SDS-PAGE, extracted from the SDS gel slices, and then ethanol precipitated. PCR was conducted with primer pair FMH792 and FMH793 and with JH642 chromosomal DNA as template. For the probes used in the gel shift assay, FMH792 and FMH793 were both radiolabeled. For radiolabeling the coding or noncoding strand, radiolabeled FMH792 and FMH793 or FMH792 and radiolabeled FMH793 were used, respectively. The PCR products were extracted by PAGE and purified by an Elutip-D minicolumn (Schleicher & Schuell, Keene, N.H.) as described in the instruction manual. Similar techniques were used to prepare a probe lacking the YdiH binding site, using primers FMH792 and FMH794. All primer sequences and positions are listed in Fig. 4A.

Gel shift assays. The *cydA* probes were prepared as described above. In each reaction, the desired concentration of protein and the probe (20,000 cpm) were incubated in buffer {25 mM PIPES [piperazine-*N*,*N*′-bis(2-ethanesulfonic acid)], pH 6.1, 25 mM NaCl, 0.5 mM DTT, 2 mM EDTA, 2 mM $MgCl_2$, 5% glycerol} for 30 min at room temperature. The samples were loaded onto a 4% polyacrylamide gel made in 1× Tris-borate-EDTA. The gel was run at 4°C for 1.5 h, vacuum dried, and detected by PhosphorImager analysis.

DNase I footprinting of the *cydA* promoter. In each reaction, required protein and the probes (20,000 cpm) were incubated at room temperature for 30 min in buffer (10 mM HEPES, pH 6.1, 50 mM NaCl, 10 mM $MgCl_2$, 1 mM EDTA, 1 mM DTT, 10% glycerol). DNase I (3 μl of 0.04 U/μl in 5 mM $MgCl_2$, 5 mM $CaCl_2$) was added to each reaction mixture, and digestion was conducted for 60 s for protein-containing samples and 30 s for protein-free samples. The reaction was stopped, and the DNA fragments were purified by phenol extraction followed by ethanol precipitation. The DNA fragments were run on a 4% polyacrylamide gel containing 7 M urea and detected by PhosphorImager analysis and/or X-ray film (Fuji) radiography.

RESULTS

Identification and characterization of *cmp* mutants. *B. subtilis* strains containing Δ*resDE* mutations grew poorly on solid TBAB medium and, with time, developed opaque segregates within the lysing Δ*resDE* colonies. These segregates had an improved growth phenotype. Pure cultures were isolated from the opaque papillae or sectors and named *cmp* mutants because they compensate for the Δ*resDE* poor growth phenotype. We asked what other Δ*resDE* phenotypes were suppressed by a *cmp* mutation (Table 3). Δ*resDE cmp* mutant strains did not produce the pink colony color on TBABG or accumulate acid, characteristics of a Δ*resDE* strain (31). They also oxidize the terminal oxidase substrate, TMPD, and sporulate similar to a wild-type strain. Previous reports (30) have shown that ResD is required for 80% of the wild-type level of alkaline phosphatase induction. We have found that strains bearing the *cmp* mutation bypass the requirement for ResD for full alkaline phosphatase induction (Table 3). However, the *cmp* mutation does not compensate for the loss of *resDE* for anaerobic growth (19–21) or *ctaA* expression (23, 38). Both *ctaA* and genes required for anaerobic growth require ResD as a transcription activator, suggesting that the nature of the *cmp* mutation is not to simply fill the role of ResD as a transcriptional regulator for Res regulon members.

Identification of Tn*10* insertions linked to the *cmp* mutation by transformation. Tn*10* mutagenesis of Δ*resDE cmp* strains was performed by using a Tn*10* insertion library generated in JH642. Transformants of the Tn*10* library into Δ*resDE cmp* strains were screened for any Tn*10* insertion close to the *cmp* locus that had cotransformed with a wild-type copy of the *cmp* gene leading to a phenotypic reversion from that of a *cmp* Δ*resDE* strain to a Δ*resDE* strain. Screening was performed as described in Materials and Methods and identified six candidate Tn*10* insertions, which were selected for further study.

Backcross transformation of chromosomal DNA from each Tn*10* into a number of Δ*resDE cmp* strains was performed to determine the proximity of each Tn*10* to the *cmp* locus. These transformations placed the candidate Tn*10* insertions in two classes. The first class, MH5882 (Tn*10-1*), was linked by backcross transformation to the *cmp* locus in 100% of the transformants screened; while the second class, MH5883 (Tn*10-2*), was linked in 70% of the transformants screened.

Additionally, we have shown that MH5882 (Δ*resDE cmp cydD*::Tn*10-1*) behaves phenotypically as a Δ*resDE* strain with regards to growth, red pigment formation, sporulation, TMPD

TABLE 3. Phenotypic characterization of mutants used in this study

Strain (relevant genotype)	Growth[a]	Red pigmentation[b]	Sporulation (%)[c]	Oxidization of TMPD[d]	Accumulation of organic acids[e]	Anaerobic growth[f]	*ctaA-lacZ* expression[g]	Alkaline phosphatase induction (%)[h]
JH642 (wild type)	+	−	50	+	−	+	+	100
MH5202 (Δ*resDE*)	+/−	+	0.9	−	+	−	−	20
MH5857 (*cmp* Δ*resDE*)	+	−	47	+	−	−	−	100
MH5893 (Ω*ydiH* Δ*resDE*)	+	−	33	+	−	−	ND[i]	100
MH5891 (Ω*ydiH*)	+	−	44	+	−	+	ND	100
MH5882 (*cydD*::Tn*10-1* Δ*resDE cmp*)	+/−	+	0.3	−	+	−	ND	20
MH5885 (Δ*resDE* P*spac-cydABCD* with IPTG)	+	−	20	+	−	−	ND	ND
MH5885 (Δ*resDE* P*spac-cydABCD* without IPTG)	+/−	+	4	−	+	−	ND	ND

[a] Growth on TBAB medium without glucose.
[b] Pink colony on TBABG medium.
[c] Percentage of colonies forming heat-resistant spores.
[d] Ability to oxidize artificial electron donor TMPD.
[e] Accumulation of organic acids on purification agar medium plates.
[f] Anaerobic growth in medium containing nitrate.
[g] Expression of a *ctaA-lacZ* fusion under phosphate-limiting conditions.
[h] Percentage of wild-type level of alkaline phosphatase induction.
[i] ND, not determined.

oxidation, acid accumulation, anaerobic growth, and alkaline phosphatase induction (Table 3). This indicates that this Tn*10* insertion is sufficient to complement the *cmp* mutation.

Tn*10-1* and Tn*10-2* are inserted approximately 75° apart on the chromosome. DNA adjacent to Tn*10-2* in MH5883 was amplified by inverse PCR and sequenced. The sequence revealed that Tn*10-2* was inserted after bp 922 of a 23S rRNA gene. To determine which of the 10 genomic copies of the 23S rRNA contained Tn*10-2*, we performed PBS1 transduction mapping, which placed Tn*10-2* in *rrnE-23S* (54.4°) between *phoB* (64% linked, 53°) and *purB* (84% linked, 56.9°).

The use of similar techniques with strain MH5882 placed Tn*10-1* after bp 316 in *cydD. cydD* is located at 339° in the *B. subtilis* genome within an operon that encodes cytochrome *bd* oxidase (*cydAB*) and a putative ABC transporter (*cydCD*) required for the transport of cytochrome *bd* ubiquinol oxidase (35). These data place Tn*10-1* and Tn*10-2* approximately 75° apart on the *B. subtilis* chromosome, indicating that both insertions cannot be cotransformed with the *cmp* locus. Because Tn*10-1* caused a reversion from the Δ*resDE cmp* phenotype to the Δ*resDE* phenotype 100% of the time, we reasoned that *cydD* and cytochrome *bd* might be essential to the *cmp* mutant phenotype and that Tn*10-2* was likely close to the *cmp* locus.

***cmp* maps to the *phoB-purB* region.** PBS1 transduction mapping showed that *phoB* (MH1562) and *purB* (1A601) cotransduced with the *cmp* locus at frequencies of 66 and 58%, respectively, indicating that the *cmp* locus was close to Tn*10-2*. The location of the *cmp* mutation was further analyzed in a three-factor cross, using MH5881 (Δ*tatCY* Δ*ydhQ*) as the donor strain and MH5857 (*cmp*) as the recipient strain, which placed the *cmp* mutation between *tatCY* and *ydhQ* (Table 4 and Fig. 1). This region contains approximately 14 kb of DNA including *rrnE-23S* (Fig. 1A). To further define the region containing the *cmp* mutation, a second three-factor cross was performed with MH5874 (Δ*tatCY rrnE-23S*::Tn*10-2*) as the donor strain and MH5857 (*cmp*) as the recipient strain (Table 4 and Fig. 1). These results clearly demonstrated that the *cmp* mutation was located between *tatCY* and *rrnE-23S* (Fig. 1B).

Each Δ*resDE cmp* strain has a mutation in YdiH. To determine the exact location and nature of the *cmp* mutation, we sequenced the 8-kb region between *rrnE-23S* and *tatCY* in MH5857 (Δ*resDE cmp*). The primers used in this sequencing

TABLE 4. Transformation mapping of the *cmp* locus[a]

Transformation recipient	Transformation donor	Transformant phenotype	Frequency (%)
MH5857(*cmp*)			
Cross 1	MH5881 (*tatCY*::Spc^r *ydhQ*::Erm^r)	Spc^{r}Erm^s*cmp*	41
		Spc^{r}Erm^s	38
		Spc^{r}Erm^r	14
		Spc^{r}Erm^r*cmp*	7
Cross 2	MH5874 (*tatCY*:Spc^r *rrnE-23s*:Kn^r)	Spc^r Kn^s	59
		Spc^r Kn^r	21
		Spc^r *cmp* Kn^s	15
		Spc^r *cmp* Kn^r	5

[a] The frequency of each transformant obtained is shown. In cross 1, three-factor cross transformation using MH5881 (Δ*ydhQ* Δ*tatCY*) as the donor strain and MH5857 (*cmp*) as the recipient strain was selected on Spc^r and screened for Erm^r and the *cmp* phenotype. In cross 2, three-factor cross transformation using MH5874 (Δ*tatCY rrnE-23s*::Tn*10-2*) as the donor strain and MH5857 (*cmp*) was selected on Spc^r and screened for Neo^r and for the *cmp* phenotype.

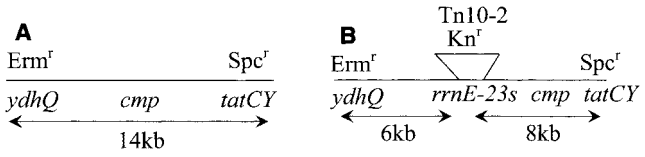

FIG. 1. Transformation mapping of the *cmp* locus. The frequency of each transformant obtained is shown in Table 4. Three-factor cross transformation using MH5881 (Δ*ydhQ* Δ*tatCY*) as the donor strain and MH5857 (*cmp*) as the recipient strain was selected on Spc^r and screened for Erm^r and the *cmp* phenotype, as shown in Table 4. Three-factor cross transformation using MH5874 (Δ*tatCY rrnE-23S*::Tn*10-2*) as the donor strain and MH5857 (*cmp*) was selected on Spc^r and screened for Neo^r and for the *cmp* phenotype, as shown in Table 4. (A) The first three-factor cross (cross 1 in Table 4) places *cmp* in the 14-kb region between *ydhQ* and *tatCY*. (B) The second three-factor cross (cross 2 in Table 4) localizes *cmp* between the Tn*10-2* insertion and *tatCY*.

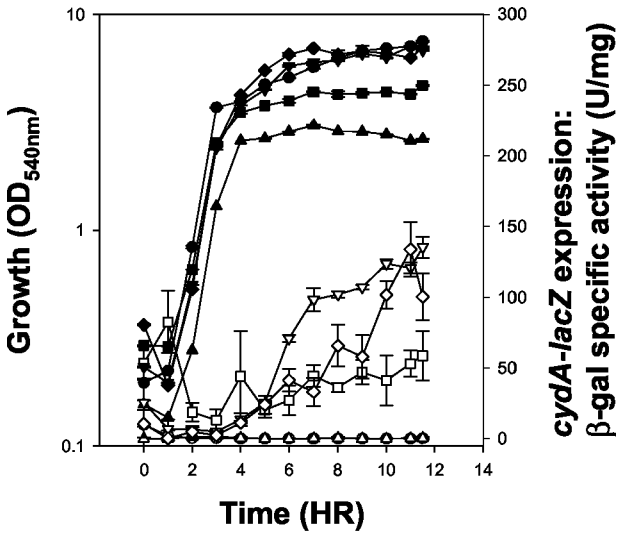

FIG. 2. Growth and *cydA-lacZ* expression from *B. subtilis* strains cultured for 11.5 h in LB medium supplemented with 0.5% glucose. Growth, solid symbols; β-galactosidase, open symbols. ●, MH5878 (wild-type *cydA-lacZ*); ▲, MH5880 (Δ*resDE cydA-lacZ*); ▼, MH5879 (Δ*resDE cmp cydA-lacZ*); ■, MH5891 (Ω*ydiH cydA-lacZ*); ◆, MH5893 (Δ*resDE* Ω*ydiH cydA-lacZ*).

are found in Table 2, and the procedure for this sequencing is described in Materials and Methods. The only alteration from the published sequence (16) in this 8-kb region of MH5857 was a 13-bp deletion 136 bp into the coding sequence of *ydiH* (Table 5).

Additional isolates of Δ*resDE* strains containing a *cmp* mutation were sequenced, yielding three additional alleles of *ydiH* (Table 5). MH5859 contained an insertion of a single A-T base pair after bp 189 of *ydiH*. MH5887 contained an A-to-T change 7 bp into *ydiH*. Finally, MH5888 contained a G-to-A change 157 bp into *ydiH*.

The mutation found in MH5857 created a frameshift after the 45th codon of *ydiH* that leads to a stop codon after 79 amino acids (aa). The mutation found in MH5859 created a frameshift after the 63rd codon of *ydiH* that placed a stop codon 4 codons later. The mutation found in MH5887 created a nonsense codon after the second codon in *ydiH*, encoding a peptide of just 2 aa. The mutation in MH5888 creates a full-length protein but has a base pair substitution at position 157 that leads to a missense mutation changing aa 53 from aspartate to asparagine. The effect of this *cmp* mutation will be nonpolar with regards to *tatAY* and *tatCY*, the genes downstream of *ydiH* in the operon. Residue 53 appears to be crucial to the protein function, and based on the results of a BLAST search, is conserved among the 10 additional members of the family of proteins that includes YdiH. This family is composed of prokaryotic DNA-binding proteins and includes p25, a recently characterized DNA-binding protein from *T. aquaticus* YT-1 (6). Together, these data suggest that the nature of the *cmp* mutation is a loss-of-function mutation in *ydiH*, a gene encoding a protein with homology to a family of AT-rich DNA-binding proteins.

A loss-of-function mutation in *ydiH* is the sole mutation responsible for the *cmp* phenotype. To determine if the loss-of-function mutation in *ydiH* found in our Δ*resDE cmp* strains is the sole mutation responsible for the *cmp* phenotype in that background, we created an independent disruption of *ydiH* (MH5891) by cloning a 516-bp internal fragment of *ydiH* into pDG1727 and transforming the plasmid to JH642 to yield MH5891. Transformation of chromosomal DNA from MH5202 (Δ*resDE*) into MH5891 (Ω*ydiH*) yielded a *resDE ydiH* double mutant strain (MH5893). The growth of MH5893 (Δ*resDE* Ω*ydiH*) was similar to that of a Δ*resDE cmp* strain on both TBAB and TBABG plates (Table 3). MH5893 (Ω*ydiH* Δ*resDE*) was phenotypically identical to the Δ*resDE cmp* strain with regard to anaerobic growth and acid accumulation, sporulation, TMPD oxidase activity, and levels of Pho induction (Table 3). The phenotypes of strains bearing a single-crossover insertion in *ydiH* (MH5891) were unchanged from that of the parent strain, JH642 (Table 3). These data confirm that the nature of the *cmp* mutation is that of a loss-of-function mutation in *ydiH*.

TABLE 5. Mutations found in *ydiH* in Δ*resDE cmp* strains

Strain	Mutation	Result
MH5888	G157 → A	Asp → Asn
MH5859	A insertion after 189	Frameshift
MH5857	Δ136–149	Frameshift
MH5887	A7→ T	Nonsense

Cytochrome *bd* is aberrantly expressed in a *cmp* mutant strain. Based on the fact that a Tn*10* insertion in *cydD* caused a suppression of the Δ*resDE cmp* phenotype to the Δ*resDE* phenotype 100% of the time, we hypothesized that cytochrome *bd* played an important role in the *cmp* phenotype. Aberrant expression of cytochrome *bd* in strains bearing mutations in *ydiH* was observed in *cydA-lacZ* fusion studies (Fig. 2). We found that a wild-type strain and a strain bearing a single mutation in *resDE* failed to express the *cydA-lacZ* fusion during stationary phase in cells grown in LB medium with 0.5% glucose. In contrast, strains bearing mutations in *ydiH*, MH5891 (Ω*ydiH cydA-lacZ*), MH5879 (Δ*resDE cmp cydA-lacZ*), and MH5893 (Δ*resDE* Ω*ydiH cydA-lacZ*), all express the *cydA-lacZ* fusion under these growth conditions. In order to confirm this aberrant expression, we examined light absorption difference (dithionite reduced minus ferricyanide oxidized)

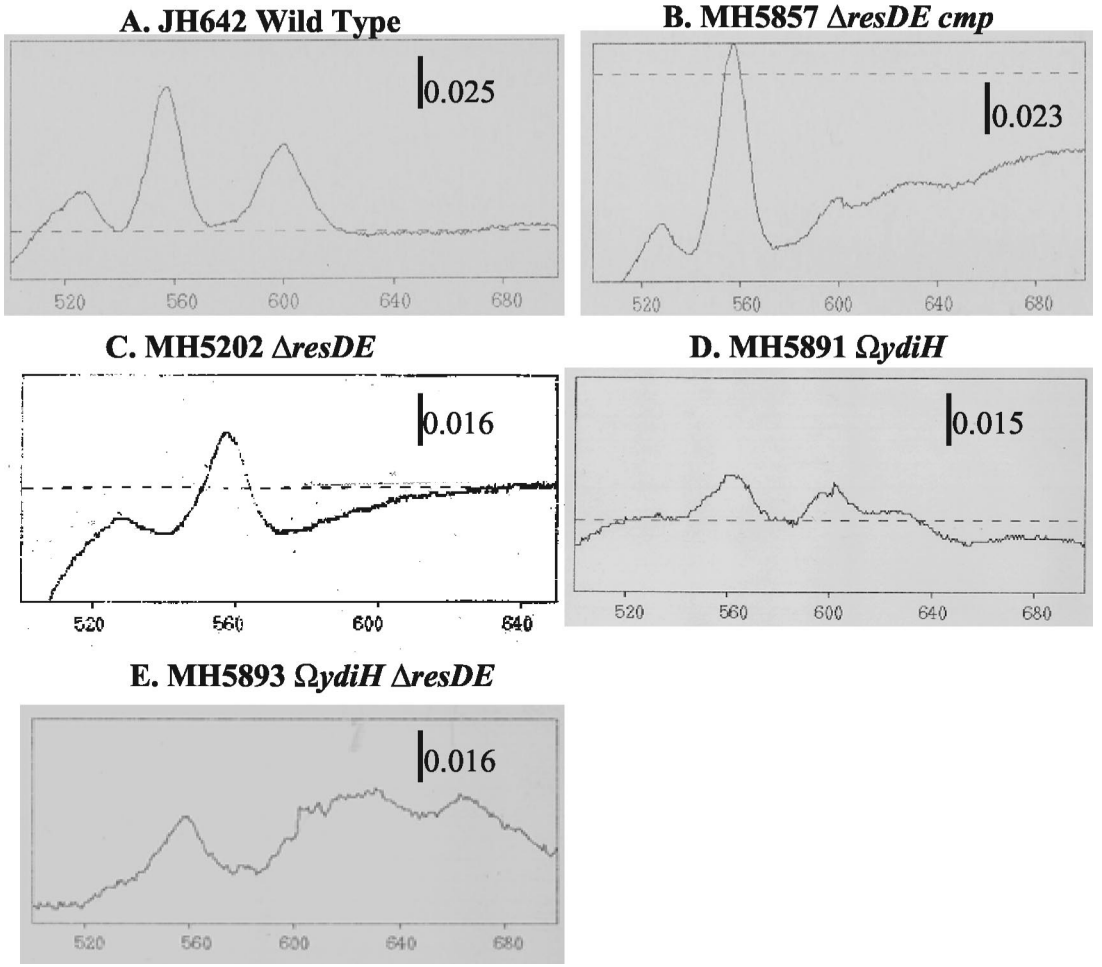

FIG. 3. Light absorption difference (dithionite reduced minus ferricyanide oxidized) spectra of membranes from strains JH642 (wild type), MH5202 (Δ*resDE*), MH5887 (Δ*resDE cmp*), MH5891 (Ω*ydiH*), and MH5893 (Ω*ydiH* Δ*resDE*). *B. subtilis* strains were grown in LB medium with 0.5% glucose and harvested during stationary phase. A representative spectrum is shown for each strain. (A) JH642. (B) MH5857. (C) MH5202. (D) MH5891. (E) MH5893.

spectra from these strains grown under the same conditions to stationary phase (Fig. 3). The aberrant expression of cytochrome *bd* in strains bearing loss-of-function mutations in *ydiH* was observed in spectra from a strain bearing the *cmp* Δ*resDE* mutation (Fig. 3B), in the parental strain containing a disruption mutation in *ydiH* (Fig. 3D), and in the *ydiH resDE* double mutant strain (Fig. 3E). Figure 3B, D, and E show the spectral pattern associated with cytochrome *bd*: that is a characteristic trough at 650 nm, a peak at 622 nm, and a peak at 595 nm that we would normally not observe in a strain bearing a Δ*resDE* mutation (Fig. 3C). This expression pattern has previously been established for a strain producing cytochrome *bd* (35). Cytochrome *bd* is not present in membranes from a wild-type strain or a Δ*resDE* strain grown under the same conditions (Fig. 3A and C, respectively). These data suggest that cytochrome *bd* is being aberrantly expressed in a *cmp* strain which bears a loss-of-function mutation in YdiH, a member of a family of DNA-binding proteins, suggesting that YdiH might function as a repressor of the *cydABCD* operon.

***ydiH* binds to the *cydA* promoter.** Winstedt et al. (35) described primer extension experiments using mRNA harvested from cells grown to the exponential-growth phase, transition phase, or stationary phase that identified a major *cydA* transcript start site located at −193 bp upstream of a translational start site. A putative SigA-dependent −10 and −35 region (Fig. 4A) was found upstream of the transcriptional start site. An inverted repeat, −114 to −107, was proposed as the binding site for regulatory protein(s) (35) (Fig. 4A). To determine if YdiH's regulation was direct or indirect, binding of YdiH to the *cydA* promoter was tested by using gel shift assays (Fig. 4B). The YdiH-*cydA* DNA complex formed at a concentration of 316 nM YdiH. An increasing concentration of YdiH led to the formation of a large-molecular-weight complex, suggesting that YdiH binds to DNA at more than one site and/or YdiH oligomerized upon DNA binding. To further understand the nature of YdiH-DNA complex, we conducted DNase I protection assays (Fig. 4C). YdiH protected three regions on either strand. The regions that were protected were −28 to −54, −60 to −86, and −88 to −122 on the coding strand and −32 to −59, −65 to −91, and −94 to −126 on the noncoding strand. The regions between these three protected regions were more sensitive to DNase I digestion than that of YdiH-free sample,

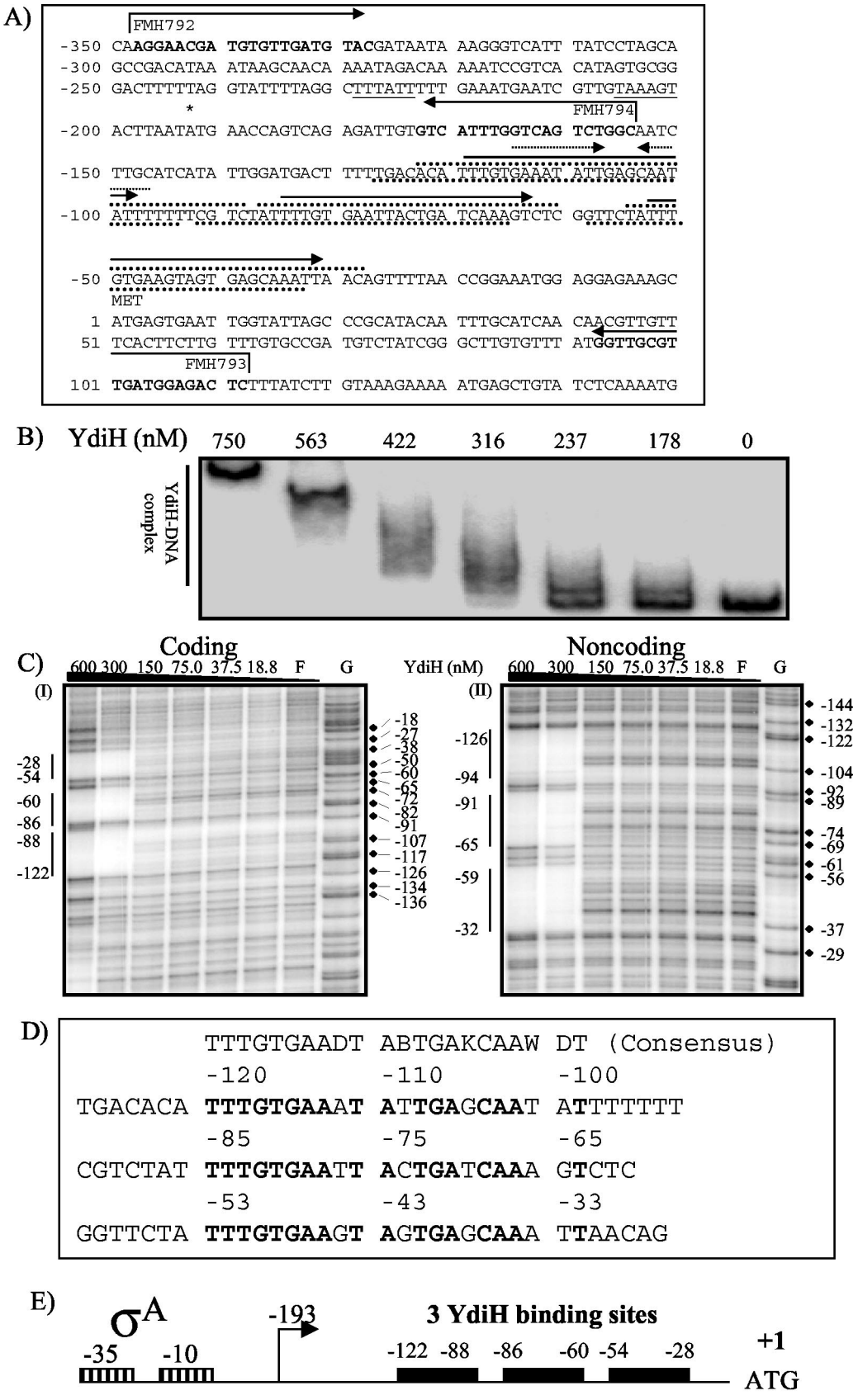
A)
FMH792
-350 CAAGGAACGA TGTGTTGATG TACGATAATA AAGGGTCATT TATCCTAGCA
-300 GCCGACATAA ATAAGCAACA AAATAGACAA AAATCCGTCA CATAGTGCGG
-250 GACTTTTTAG GTATTTTAGG CTTTATTTTT GAAATGAATC GTTGTAAAGT
*
FMH794
-200 ACTTAATATG AACCAGTCAG AGATTGTGTC ATTTGGTCAG TCTGGCAATC
-150 TTGCATCATA TTGGATGACT TTTTGACACA TTTGTGAAAT ATTGAGCAAT
-100 ATTTTTTTCG TCTATTTTGT GAATTACTGA TCAAAGTCTC GGTTCTATTT
-50 GTGAAGTAGT GAGCAAATTA ACAGTTTTAA CCGGAAATGG AGGAGAAAGC
MET
1 ATGAGTGAAT TGGTATTAGC CCGCATACAA TTTGCATCAA CAACGTTGTT
51 TCACTTCTTG TTTGTGCCGA TGTCTATCGG GCTTGTGTTT ATGGTTGCGT
FMH793
101 TGATGGAGAC TCTTTATCTT GTAAAGAAAA ATGAGCTGTA TCTCAAAATG
B)
YdiH (nM)
750
563
422
316
237
178
0
YdiH-DNA complex
C)
Coding
600 300 150 75.0 37.5 18.8 F G
(I)
-28
-54
-60
-86
-88
-122
-18
-27
-38
-50
-60
-65
-72
-82
-91
-107
-117
-126
-134
-136
YdiH (nM)
Noncoding
600 300 150 75.0 37.5 18.8 F G
(II)
-126
-94
-91
-65
-59
-32
-144
-132
-122
-104
-92
-89
-74
-69
-61
-56
-37
-29
D)
TTTGTGAADT ABTGAKCAAW DT (Consensus)
-120 -110 -100
TGACACA TTTGTGAAAT ATTGAGCAAT ATTTTTTT
-85 -75 -65
CGTCTAT TTTGTGAATT ACTGATCAAA GTCTC
-53 -43 -33
GGTTCTA TTTGTGAAGT AGTGAGCAAA TTAACAG
E)
σA
-193
3 YdiH binding sites
-35 -10
-122 -88 -86 -60 -54 -28
+1
ATG

indicating these regions were exposed due to YdiH binding. Further DNA sequence analysis revealed three tandem 22-bp repeats, −120 to −109, −85 to −64, and −53 to −32, with a consensus sequence, 5′-TTTGTGAA(A/T/G)TA(T/C/G)TGA (G/T)CAA(A/T)(A/T/G)T-3′ (Fig. 4D). Additional gel shift assays using a *cydA* promoter probe (PCR product of primers FMH792 and FMH794, Fig. 4A) that lacks the YdiH binding site, showed no YdiH-*cydA* complex formation when YdiH concentrations as high as 1 μM were used (data not shown). A graphical description of YdiH binding relative to all transcription and translation start sites is found in Fig. 4E.

Cytochrome *bd* is sufficient to create the *cmp* mutant phenotype. In order to confirm the role of cytochrome *bd* in the *cmp* phenotype, we created a strain in which the *cydABCD* operon was under the control of an inducible promoter (P_{spac}) in a Δ*resDE* background (MH5885). We then asked if expression of cytochrome *bd* in this background would be sufficient to create the phenotypes associated with a *cmp* Δ*resDE* strain. We found that induction of cytochrome *bd* was sufficient to compensate for the loss of ResD for all phenotypes normally associated with the *cmp* mutation (Table 3). The same strain grown without induction of cytochrome *bd* mimicked the phenotype of a Δ*resDE* strain (Table 3).

DISCUSSION

In this report, we have shown that spontaneous mutations arise in *B. subtilis resDE* strains that compensate for the loss of ResD for all known phenotypes that are not associated with ResD's role as a transcriptional activator. Previous reports (7) have demonstrated that strains deficient in CcdA, which is proposed to play a role in keeping two critical cysteinyls in apocytochrome *C* reduced, can pick up secondary mutations in either *bdbC* or *bdbD* which code for thiol-disulfide oxidoreductases. These secondary mutations complement the loss of CcdA for a number of phenotypes. An additional report (25) demonstrated that *Bacillus stearothermophilus* strains deficient in cytochrome caa_3 have the ability to spontaneously produce cytochrome *bd*. It was proposed that this takes place due to a mutation in a repressor of the operon that produces cytochrome *bd*. However, the nature of this mutation has not been described to date.

The *cmp* mutation in a *B. subtilis* Δ*resDE* background is a loss-of-function mutation in *ydiH*. YdiH has been assigned to a family of AT-rich DNA-binding proteins based on sequence homology (16). Included in this family is p25, a protein from *T. aquaticus* YT-1 that has been recently characterized (6) and was shown to bind AT-rich DNA segments within its regulatory regions. During the course of characterizing the *cmp* mutation, we determined that cytochrome *bd* was aberrantly expressed in a Δ*resDE cmp* background (Fig. 2 and 3B), suggesting that YdiH may serve as a negative regulator of the *cydABCD* operon. We propose that this regulation is direct based on the results of our gel-shift and DNase I protection data (Fig. 4).

The 22-bp conserved repeats that were protected by YdiH binding (Fig. 4D) suggested that YdiH may bind DNA as a dimer to protect this relatively long region, equal to two turns of the helix. The YdiH homologue protein, p25, an AT-rich DNA-binding protein from *T. aquaticus* YT-1, is a dimer in solution (6).

The gel-shift pattern of the *cydA* promoter with increasing concentrations of YdiH suggested that multiple complexes were formed, a fact that was supported by DNase I protection at three sites on the *cydA* promoter by YdiH (Fig. 4B and C). The 10 to 13 bp between the direct repeats (each approximately equal to one turn of the helix) were apparently bent due to YdiH binding as they were hypersensitive to DNase I digestion. Low concentrations of YdiH initially bound to the −88 to −122 region (Fig. 4C) followed by simultaneous protection of two downstream binding sites at increasing concentrations. This may suggest sequential and/or cooperative binding of YdiH to the *cydA* promoter, which may be important for YdiH's function as a repressor. The *cydA* promoter region contains a long untranslated region of 193 bp, a length similar to the leader transcript for the *trpE* operon (11, 27). The data presented here are consistent with a repressor function for YdiH, which binds at three sites 71 bp downstream of the transcriptional start site. Transcription from the *cydA* promoter likely proceeds through the initial 71 bp until RNA polymerase encounters YdiH, leading to a loss of production of functional cytochrome *bd*. Thus, one of the functions of this untranslated region is to allow for repression of transcription of the operon.

In characterizing the Δ*resDE cmp* strain, we found that all phenotypes associated with a *resDE* mutation are suppressed by the *cmp* mutation except for *ctaA* expression and anaerobic growth, two phenotypes associated with ResD's role as a tran-

FIG. 4. YdiH binds directly to the *cydA* promoter. (A) Structure of the *cydA* regulatory region. The major transcriptional start site is shown with an asterisk. The inverted repeats and tandem repeats are indicated as dotted line arrows or solid arrows, respectively. The YdiH protected regions revealed by the DNase I footprinting assay are shown by dotted lines above (coding strand) and below (noncoding strand) the sequence. The consensus sequences for the −35 and −10 σ^A recognition sequences are underlined. The primer sequences used to generate PCR products are in boldface, and broken arrows indicate the 5′-to-3′ sequence. The numbering is relative to the translation start (ATG) as +1 (also for panels C and D). (B) Gel shift assay of the *cydA* promoter with YdiH. The probe was the PCR product using radiolabeled primers FMH792 and FMH793 and JH642 chromosomal DNA as template. The primer was labeled as described in Materials and Methods. The concentrations of YdiH used are indicated at the top of each lane. (C) DNase I footprinting of the *cydA* promoter by using YdiH. Labeled DNA fragments were generated as in panel B. For the coding or noncoding footprint, FMH792 or FMH793 was end labeled, respectively. The YdiH concentrations are shown at the top of each lane. F, free of YdiH; G, Maxam-Gilbert G-sequencing reaction lane as a marker. The vertical lines show the YdiH protected regions. (D) The *cydA* promoter alignment for directed repeats. The consensus sequence is shown above, and the IUPAC (the International Union of Pure and Applied Chemistry) ambiguity codes for DNA were used: D = A, T, or G; B = T, C, or G; K = G or T; and W = A or T. The identical base pairs among the three repeats are in bold. (E) Graphic representation of YdiH binding on the *cydA* promoter. Solid black boxes represent the three YdiH binding site on the *cydA* promoter region. The boxes with vertical lines represent the consensus −10 and −35 for σ^A identified previously (35). The numbering is relative to the translational start (ATG) as +1. For simplicity, only coding strand protected regions are numbered. The transcription start site is identified with a broken arrow.

scriptional activator (Table 3). This suggests that the role of the *cmp* mutation is not to simply create a mechanism to bypass the activity of ResD in the cell as a transcriptional activator. Rather, it is the expression of cytochrome *bd* that is responsible for the phenotypic changes associated with a *cmp* mutation. This hypothesis is strongly supported in our studies with MH5885 (Δ*resDE* P_{spac}-*cydABCD*). In the presence of IPTG, this strain expressed the *cydABCD* operon and behaved phenotypically as a strain bearing a *cmp* mutation. In the absence of IPTG, this strain behaves in a manner similar to a Δ*resDE* strain (Table 3). In the case of sporulation, previous work (34) has suggested that a heme-copper oxidase (either aa_3 or caa_3) is required for efficient sporulation. However, these sporulation assays were performed in NSMP medium, a medium in which cytochrome *bd* is poorly expressed (35). Our Δ*resDE* strains, which cannot make cytochrome aa_3 or caa_3, are sporulation defective; however, the *cmp* Δ*resDE* double mutants that aberrantly express cytochrome *bd* sporulate at wild-type levels, suggesting that either a heme-copper oxidase or cytochrome *bd* is sufficient to allow for efficient sporulation.

In an effort to characterize the gene expression patterns of *B. subtilis* under various respiratory conditions, Ye et al. performed microarray analysis on a strain bearing a *resDE* mutation grown under aerobic respiratory conditions in 2× YT medium supplemented with 1% glucose and 20 mM K_3PO_4 (36). They found that the *cydABCD* operon was induced in a strain bearing a *resDE* mutation compared to the wild-type strain. A possible explanation for this discrepancy is that during the course of study, their *resDE* strain acquired a *cmp* mutation (a frequent phenomenon), leading to aberrant expression of the *cydABCD* operon. Our studies using 2× YT medium supplemented with 1% glucose and 20 mM K_3PO_4 demonstrated that *cydA-lacZ* expression was reduced in a Δ*resDE* strain in comparison to that in the wild-type strain (data not shown).

Our analysis of *B. subtilis* strains bearing *cmp* mutations has provided insight into the function of YdiH. Based on the fact that the *cmp* mutation appears to be a loss-of-function mutation in *ydiH* (putative DNA-binding protein) and that strains bearing the *cmp* mutation aberrantly express cytochrome *bd*, we proposed that YdiH functions as a negative regulator for *cydABCD* expression. DNA-binding assays have demonstrated that YdiH directly binds the *cydABCD* promoter region. This binding takes place at three tandem repeats which are separated by 10 to 13 bp. These direct repeats are located in the long untranslated region of the *cydABCD* promoter. The aberrant expression of cytochrome *bd* in a Δ*resDE* background is sufficient to suppress the phenotypes associated with the loss of cyotochromes aa_3 and caa_3 in this background. Future studies will determine how *cmp* mutations bypass the requirement for ResD for full alkaline phosphatase induction (30) and what insight we can gain from our understanding of the *cmp* mechanism into the role of ResD in alkaline phosphatase induction, where it is normally required for 80% of the wild-type alkaline phosphatase response.

ACKNOWLEDGMENTS

This work was supported by National Institutes of Health grant GM-33471 to F.M.H.

We thank Jörg Müller, Nick Kapp, Ruth Chestnut, and Gufou Sun for strains. We thank the *Bacillus* genetic stock center for PBS1 phage.

REFERENCES

1. **Bisschop, A., and W. N. Konings.** 1976. Reconstitution of reduced nicotinamide adenine dinucleotide oxidase activity with menadione in membrane vesicles from the menaquinone-deficient *Bacillus subtilis aroD.* Relation between electron transfer and active transport. Eur. J. Biochem. **67:**357–365.
2. **Carls, R. A., and R. S. Hanson.** 1971. Isolation and characterization of tricarboxylic acid cycle mutants of *Bacillus subtilis.* J. Bacteriol. **106:**848–855.
3. **Chary, V. K., E. I. Amaya, and P. J. Piggot.** 1997. Neomycin- and spectinomycin-resistance replacement vectors for *Bacillus subtilis.* FEMS Microbiol. Lett. **153:**135–139.
4. **Cutting, S. M., and P. B. Vander Horn.** 1990. Genetic analysis, p. 24–74. *In* C. R. Harwood and S. M. Cutting (ed.), Molecular biological methods for *Bacillus.* John Wiley & Sons, Inc., New York, N.Y.
5. **de Vrij, W., B. van den Burg, and W. N. Konings.** 1987. Spectral and potentiometric analysis of cytochromes from *Bacillus subtilis.* Eur. J. Biochem. **166:**589–595.
6. **Du, X., and J. J. Pene.** 1999. Identification, cloning and expression of p25, an AT-rich DNA-binding protein from the extreme thermophile, Thermus aquaticus YT-1. Nucleic Acids Res. **27:**1690–1697.
7. **Erlendsson, L. S., and L. Hederstedt.** 2002. Mutations in the thiol-disulfide oxidoreductases BdbC and BdbD can suppress cytochrome *c* deficiency of CcdA-defective *Bacillus subtilis* cells. J. Bacteriol. **184:**1423–1429.
8. **Ferrari, E., S. M. H. Howard, and J. A. Hoch.** 1986. Effect of stage 0 sporulation mutations on subtilisin expression. J. Bacteriol. **166:**173–179.
9. **Guerout-Fleury, A. M., K. Shazand, N. Frandsen, and P. Stragier.** 1995. Antibiotic-resistance cassettes for *Bacillus subtilis.* Gene **167:**335–336.
10. **Hanahan, D.** 1985. Techniques for transformation of *E. coli*, p. 109–135. *In* D. M. Glover (ed.), DNA cloning II. A practical approach. IRL Press, Washington, D.C.
11. **Henner, D. J., L. Band, and H. Shimotsu.** 1985. Nucleotide sequence of the *Bacillus subtilis* tryptophan operon. Gene **34:**169–177.
12. **Homuth, G., A. Rompf, W. Schumann, and D. Jahn.** 1999. Transcriptional control of *Bacillus subtilis hemN* and *hemZ.* J. Bacteriol. **181:**5922–5929.
13. **Hulett, F. M., C. Bookstein, and K. Jensen.** 1990. Evidence for two structural genes for alkaline phosphatase in *Bacillus subtilis.* J. Bacteriol. **172:**735–740.
14. **Jongbloed, J. D., U. Martin, H. Antelmann, M. Hecker, H. Tjalsma, G. Venema, S. Bron, J. M. van Dijl, and J. Muller.** 2000. TatC is a specificity determinant for protein secretion via the twin-arginine translocation pathway. J. Biol. Chem. **275:**41350–41357.
15. **Kapp, N.** 1992. Analysis of the phosphate stimulon of *Bacillus subtilis.* Ph.D. thesis. University of Illinois at Chicago, Chicago.
16. **Kunst, F., N. Ogasawara, I. Moszer, A. M. Albertini, G. Alloni, V. Azevedo, M. G. Bertero, P. Bessieres, A. Bolotin, S. Borchert, R. Borriss, L. Boursier, A. Brans, M. Braun, S. C. Brignell, S. Bron, S. Brouillet, C. V. Bruschi, B. Caldwell, V. Capuano, N. M. Carter, S. K. Choi, J. J. Codani, I. F. Connerton, A. Danchin, et al.** 1997. The complete genome sequence of the gram-positive bacterium *Bacillus subtilis.* Nature **390:**249–256.
17. **Liu, X., and H. W. Taber.** 1998. Catabolite regulation of the *Bacillus subtilis ctaBCDEF* gene cluster. J. Bacteriol. **180:**6154–6163.
18. **Mueller, J. P., and H. W. Taber.** 1989. Isolation and sequence of *ctaA*, a gene required for cytochrome aa_3 biosynthesis and sporulation in *Bacillus subtilis.* J. Bacteriol. **171:**4967–4978.
19. **Nakano, M. M., T. Hoffmann, Y. Zhu, and D. Jahn.** 1998. Nitrogen and oxygen regulation of *Bacillus subtilis nasDEF* encoding NADH-dependent nitrite reductase by TnrA and ResDE. J. Bacteriol. **180:**5344–5350.
20. **Nakano, M. M., G. Zheng, and P. Zuber.** 2000. Dual control of *sbo-alb* operon expression by the Spo0 and ResDE systems of signal transduction under anaerobic conditions in *Bacillus subtilis.* J. Bacteriol. **182:**3274–3277.
21. **Nakano, M. M., Y. Zhu, M. Lacelle, X. Zhang, and F. M. Hulett.** 2000. Interaction of ResD with regulatory regions of anaerobically induced genes in *Bacillus subtilis.* Mol. Microbiol. **37:**1198–1207.
22. **Nicholson, W., and P. Setlow.** 1990. Sporulation, germination, and outgrowth, p. 391–450. *In* C. R. Harwood and S. M. Cutting (ed.), Molecular biological methods for *Bacillus.* John Wiley & Sons, Inc., New York, N.Y.
23. **Paul, S., X. Zhang, and F. M. Hulett.** 2001. Two ResD-controlled promoters regulate *ctaA* expression in *Bacillus subtilis.* J. Bacteriol. **183:**3237–3246.
24. **Perkins, J. B., A. Sloma, T. Hermann, K. Theriault, E. Zachgo, T. Erdenberger, N. Hannett, N. P. Chatterjee, V. Williams II, G. A. Rufo, Jr., R. Hatch, and J. Pero.** 1999. Genetic engineering of *Bacillus subtilis* for the commercial production of riboflavin. J. Ind. Microbiol. Biotechnol. **22:**8–18.
25. **Sakamoto, J., A. Matsumoto, K. Oobuchi, and N. Sone.** 1996. Cytochrome *bd*-type quinol oxidase in a mutant of *Bacillus stearothermophilus* deficient in *caa3*-type cytochrome *c* oxidase. FEMS Microbiol. Lett. **143:**151–158.
26. **Santana, M., F. Kunst, M. F. Hullo, G. Rapoport, A. Danchin, and P. Glaser.** 1992. Molecular cloning, sequencing, and physiological characterization of the *qox* operon from *Bacillus subtilis* encoding the *aa3*-600 quinol oxidase. J. Biol. Chem. **267:**10225–10231.
27. **Shimotsu, H., and D. J. Henner.** 1984. Characterization of the *Bacillus*

subtilis tryptophan promoter region. Proc. Natl. Acad. Sci. USA **81:**6315–6319.

28. **Shimotsu, H., and D. J. Henner.** 1986. Construction of a single-copy integration vector and its use in analysis of regulation of the *trp* operon of *Bacillus subtilis.* Gene **43:**85–94.
29. **Steinmetz, M., and R. Richter.** 1994. Easy cloning of mini-Tn*10* insertions from the *Bacillus subtilis* chromosome. J. Bacteriol. **176:**1761–1763.
30. **Sun, G., S. M. Birkey, and F. M. Hulett.** 1996. Three two-component signal-transduction systems interact for Pho regulation in *Bacillus subtilis.* Mol. Microbiol. **19:**941–948.
31. **Sun, G., E. Sharkova, R. Chesnut, S. Birkey, M. F. Duggan, A. Sorokin, P. Pujic, S. D. Ehrlich, and F. M. Hulett.** 1996. Regulators of aerobic and anaerobic respiration in *Bacillus subtilis.* J. Bacteriol. **178:**1374–1385.
32. **Trieu-Cuot, P., C. Poyart-Salmeron, C. Carlier, and P. Courvalin.** 1990. Nucleotide sequence of the erythromycin resistance gene of the conjugative transposon Tn1545. Nucleic Acids Res. **18:**3660.
33. **Vandeyar, M. A., and S. A. Zahler.** 1986. Chromosomal insertions of Tn*917* in *Bacillus subtilis.* J. Bacteriol. **167:**530–534.
34. **Winstedt, L., and C. von Wachenfeldt.** 2000. Terminal oxidases of *Bacillus subtilis* strain 168: one quinol oxidase, cytochrome aa_3 or cytochrome *bd*, is required for aerobic growth. J. Bacteriol. **182:**6557–6564.
35. **Winstedt, L., K.-I. Yoshida, Y. Fujita, and C. von Wachenfeldt.** 1998. Cytochrome *bd* biosynthesis in *Bacillus subtilis*: characterization of the *cydABCD* operon. J. Bacteriol. **180:**6571–6580.
36. **Ye, R. W., W. Tao, L. Bedzyk, T. Young, M. Chen, and L. Li.** 2000. Global gene expression profiles of *Bacillus subtilis* grown under anaerobic conditions. J. Bacteriol. **182:**4458–4465.
37. **Zamboni, N., N. Mouncey, H. P. Hohmann, and U. Sauer.** 2003. Reducing maintenance metabolism by metabolic engineering of respiration improves riboflavin production by *Bacillus subtilis.* Metab. Eng. **5:**49–55.
38. **Zhang, X., and F. M. Hulett.** 2000. ResD signal transduction regulator of aerobic respiration in *Bacillus subtilis*: *ctaA* promoter regulation. Mol. Microbiol. **37:**1208–1219.